Method of Moment simulation of full Arctic Weather Satellite structure

Roland Albers*, Mustafa Murat Bilgic†, Mark Whale†, Axel Murk*
*University of Bern, Institute of Applied Physics, Bern, Switzerland, roland.albers@unibe.ch
†TICRA, Copenhagen, Denmark, www.ticra.com

***Abstract*—The Arctic Weather Satellite is a single payload prototype for a meteorological constellation of SmallSats called EPS-Sterna. Previous analysis showed that the Arctic Weather Satellite radiometer suffers from significant spillover in the 54 GHz band. To accurately model the scattering of the spillover, new analysis using method of moments was conducted including the structure of the instrument. This paper details the results of these simulations and the resulting mitigation of the spillover.**

***Index Terms*—antennas, electromagnetics, propagation, physical optics, method of moments, quasi-optics, millimeter-wave.**

I. Introduction

The Arctic Weather Satellite (AWS) mission is a prototype for a European constellation of meteorological smallsats called EPS-Sterna. Its single payload is a cross-track scanning radiometer operating in the 50-57, 89, 165-183 and 325 GHz frequency bands. These bands provide measurements for temperature, liquid water content, precipitation and water vapour content across 19 channels. EPS-Sterna's purpose is to improve global numerical weather prediction by supplementing existing radiometer data from the large meteorological programmes such as EUMETSAT's MetOp and NOAA's JPSS. By using a smallsat constellation, more frequent measurements (sub 2 hour in the higher latitudes) than the aforementioned programmes can be provided, but this requires a compact radiometer to fit the platform. This is achieved by using a splitblock feedcluster, directly illuminating the rotating scan mirror. The general overview of the radiometer and its on-ground calibration scheme can be found in [1]. The key feature of this design approach is spillover management, as no horn in the feedcluster is sitting directly in the focus of the primary mirror. A detailed study of the optics and their performance characteristics has been performed [2] which minimised spillover variation as a function of scan mirror position but the overall spillover values for the lower bands are still significant. In the previous study, the key optical elements were analysed using the physical optics (PO) solver in GRASP. The work presented here is a detailed platform scattering analysis using the MoM/MLFMM solver in ESTEAM. GRASP and ESTEAM are specialised asymptotic and method of moment solvers, respectively, that are available in the TICRA Tools 23.0 [3] framework.

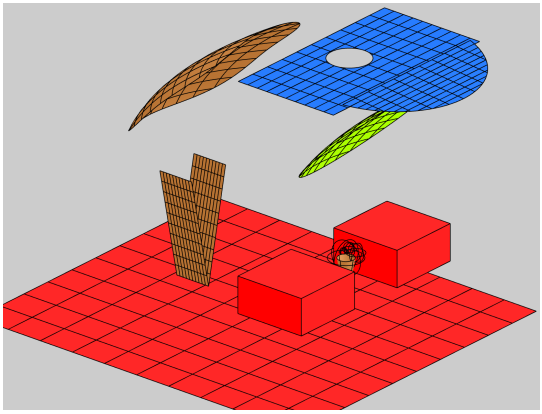

Fig. 1. PO setup in GRASP. Primary scanning reflector shown in green, roof plus angled circular element in blue. Feed cluster is located between the boxes. Red elements for illustration only.

II. Simulation Setup

A. PO model vs CAD model

The original simulation setup can be seen in Fig. 1. The only structural component included in the simulation was the roof immediately over the primary reflector which was drawn in GRASP. This part of the structure was crucial to determining if the first sidelobe of the reflector could be captured and sufficient as only the first reflection was considered. However, when examining the other parts of the spillover which are not the first sidelobe, the GRASP setup is lacking the required detail. Since the structure is metallic, it can be assumed that the majority of the spillover will not be terminated inside the instrument but will (after many reflections) be scattered into cold space or towards earth. If this spillover is not compensated for, it introduces a significant error of up to 1-2 Kelvin in Brightness temperature. Therefore it was necessary to implement a reduced model of the entire structure in the simulation. Fig. 2 shows the final model that was used for the simulations. The faces highlighted in red are covered in absorber, which was added to suppress the spillover being reflected to earth.

B. Physical Optics vs Method of Moments

This section describes the fundamental differences between PO and MoM approaches within the TICRA Tools framework and does not consider their full implementation. The PO approach within GRASP considers the scattering of a single

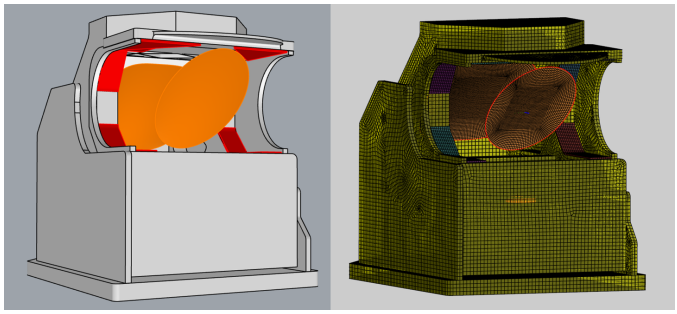

Fig. 2. CAD model of AWS radiometer used in ESTEAM. Absorber sheets shown in red.

component which is illuminated by an incident magnetic field. The scatterer can be a perfect electric conductor (PEC) or have some dielectric properties but in the context of this work only PEC was used. Using PO, the surface current of a point on a curved scatterer is equivalent to that of an infinite planar surface tangential to the scatterer surface at that point [3]. This approximation is valid for scatterers which are large in terms of wavelength. The induced currents on a PEC infinite planar scatterer (J^e_{total}) are calculated using:

$$J^e_{total} = 2\hat{n} \times \sum_{n=1} H^{inc}_n, \tag{1}$$

where H^{inc}_n is an arbitrary incident magnetic field from a source and $\hat{n}$ is the surface normal. A source in the context of GRASP can be any radiating device or another scatterer where the induced currents on it have already been calculated. Although it is possible to calculate multiple reflections with the PO approach, each reflection has to be setup manually. In the case of the AWS structure, where a large number of reflections between many components is anticipated, this is not feasible.

MoM is a numerical method to solving full-wave integral equations [4]. This allows for multiple reflections since scatterers are not treated as isolated entities like in PO. Instead, all surface currents of all scatterers are calculated at the same time. The MoM/MLFMM solver in ESTEAM discretises the geometry using higher-order quadrilateral patches and surface currents using higher-order basis functions, which reduces the required memory ($NlogN$) and time (N^3) compared to a direct solution (N^2 and N^3, respectively). However, the computational effort is still much greater than using PO and places a heavy constraint on the extent of possible simulations.

III. Simulation Results

Due to time constraints and the aforementioned computational cost, only results for the 54 GHz low band are shown here, where spillover is most relevant. Simulations were performed for nadir, $\pm 66°$, $\pm 90°$ and $180°$ scan angles and for low (50.3 GHz), mid (53.6 GHz) and high (57.3 GHz) band. Furthermore, the impact of the absorber added to the structure (Fig. 2) was also assessed by performing the scan angle sweep with and without it.

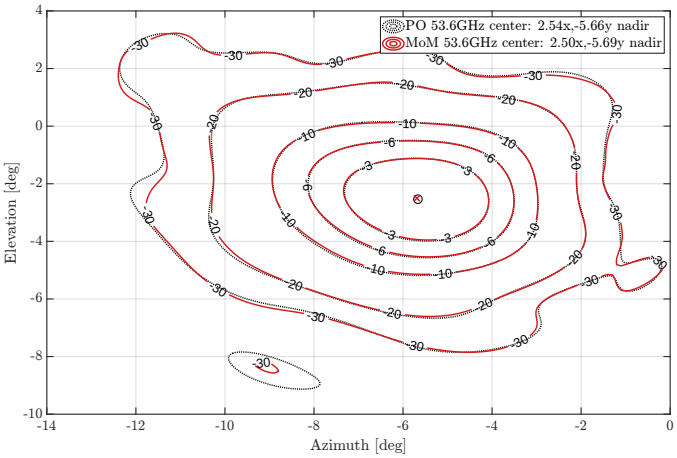

Fig. 3. Comparison between PO (dotted black) and MoM (red) mainbeam for 54 GHz mid band.

A. Mainbeam comparison

Given that the MoM simulations are understood to provide the most accurate results, it is of interest to compare these simulations results against the equivalent PO simulation results. As the simulation setup is not identical, the only meaningful comparison is the mainbeam, which predominantly depends on the feedhorn and reflector. Since both of these elements are unchanged, any differences should be due to the method used. Fig. 3 shows that there are no significant differences in the mainbeam contours down to -30dB. At -30dB some changes can be seen which is likely due to the structure and outside the mainbeam definition.

B. Scattering of structure

Fig. 4 shows the effect of including the structure on the nadir hemisphere. Nadir of the satellite is in the origin of both plots. The white line corresponds to the viewing angle of 66° off nadir which is equivalent to the earth outline. Any sidelobes within the outline will see earth which varies drastically in brightness temperature throughout the orbit. Flight direction is towards the upper boundary of the plot. Predictably, there is more low level background scattering in the forward facing hemisphere when including the structure, which is only open towards nadir. The simulation without structure does still include the circular roof (as shown in Fig. 1) and its effect is consistent between the two simulations. Including more of the upper structure (left plot) reduces the direct spillover (top left of both plots). Two scattering lobes can be seen in the left plot near the mainbeam, which were not visible without the structure. Such lobes in the earthview are significant error contributors.

C. First spillover sidelobe

The circular part of the roof structure (Fig. 2) is angled downwards by 5° and designed to deflect the first spillover sidelobe sufficiently so it does not see earth but cold sky. Alternatively, the sidelobe could be terminated using absorber. However, the thermal environment of this part of the structure

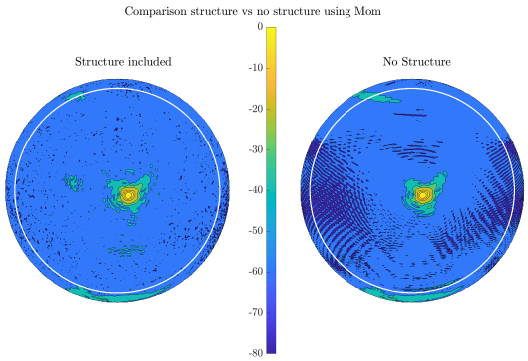

Fig. 4. Comparison of nadir hemisphere with (left) and without (right) structure. White line denotes outline of earth from satellite perspective.

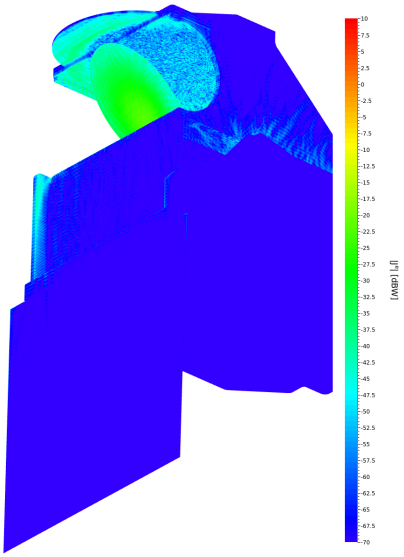

Fig. 5. Surface currents on the instrument structure and satellite frontplate. Colorbar range from -70 dB to 10 dB.

is not controlled and will change significantly throughout each orbit. This means the brightness temperature of this termination will vary continuously and will be harder to correct for than cold sky. With the full structure included, it can be confirmed that the sidelobe is not scattered by another component and deflected as intended. An additional plate representing the satellite platform below the instrument was included for a more comprehensive check. In fig. 5, showing surface currents on the structure and platform, it is apparent that the spillover is not scattered by the nadir facing surfaces of the instrument or satellite platform.

D. Impact of absorber on spillover

Absorber panels are mounted on the outward faces of the structure to terminate the scattering lobes discussed in section III-B. Fig. 6 shows a comparison of the nadir hemisphere with and without the absorber on the structure. The mainbeam has been excluded and the remaining power over the sphere

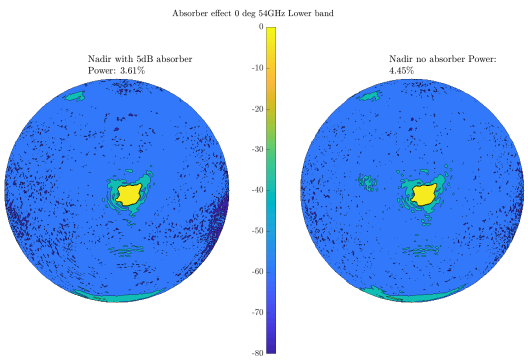

Fig. 6. Comparison of absorber on nadir hemisphere. Yellow area (mainbeam) excluded from power integral.

is integrated. Anything inside the -30dB contour around the peak gain is defined as the mainbeam. Adding the absorber is equivalent to spillover reduction of 0.84% over the entire hemisphere for the 54 GHz lower band. Other receivers have less spillover and therefore the expected reduction will be less as well.

IV. Conclusion

Previous simulation work using physical optics based simulations showed that there is significant spillover in the optics of the AWS radiometer at lower frequencies. To study where this spillover is scattered to in detail, a simplified CAD model of the AWS radiometer was included in new method of moment simulations. Full sphere farfield analysis of the 54 GHz band shows that the structure causes scattering in earth view, not previously seen. These scattering lobes were reduced by adding absorbing materials on the instrument structure which will improve instrument performance during operation.

Acknowledgement

Many thanks to Rasmus Augustsson for simplifying the CAD model of the instrument and preparing it for the ES-TEAM import. Thanks also go to TICRA for providing fast computing capacity as well as their expertise.

References

[1] R. Albers, M. Kotiranta, A. Emrich, and A. Murk, "Optical design of arctic weather satellite microwave sounder," in *2023 17th European Conference on Antennas and Propagation (EuCAP)*, 2023, pp. 1–4.
[2] R. Albers, A. Emrich, and A. Murk, "Antenna design for the arctic weather satellite microwave sounder," *IEEE Open Journal of Antennas and Propagation*, vol. 4, pp. 686–694, 2023.
[3] *TICRA Tools User's manual v23.0*, 2023.
[4] W. Gibson C., *The Method of Moments in Electromagnetics*. Chapman Hall/CRC, 2008, ch. 3.